UAV FLYING WING WITH A PHOTOVOLTAIC SYSTEM

Vasile PRISACARIU

"Henri Coandă" Air Force Academy, Brașov, Romania

DOI: 10.19062/1842-9238.2019.17.1.8

Abstract: *Unmanned aircraft have numerous operational advantages that they recommend, and flight autonomy is important in conditions of use in hostile operating environments. A method of maximizing autonomy is the use of correlated photovoltaic energy with an optimized design depending on the type of mission.*

The article presents both theoretically and numerically a technical solution for the FW-UAV using a photovoltaic system.

Keywords: *flexible solar cells, flying wing, equivalent circuit, software simulation.*

1. ACTUAL STAGE OF THE PHOTOVOLTAIC CONCEPT ON FLEXIBLE SUPPORT

Mechanically flexible solar cells could change how electricity is generated in the future. Some of the applications include the use of integrated cells in high-altitude and telecommunication space such as unmanned aerial UAVs. Photovoltaic powered flight is not a new concept, dating from 1974, the crewed aircraft - Solar Impulse, see FIG. 1 [1, 2].

FIG. 1. Solar Impulse

These flights were important due to the demonstration of night-time energy storage and flying capacity as well as increased confidence in photovoltaic technologies.

According to specialty studies [3, 4, 5], the use of photovoltaic panels in UAVs confirms the maturity of the technical solution to increase flight autonomy, here we can recall a number of projects, such as: NASA Pathfinder in 1983 (Figure 2a); and Sunseeker in 1990 (FIG. 2b).

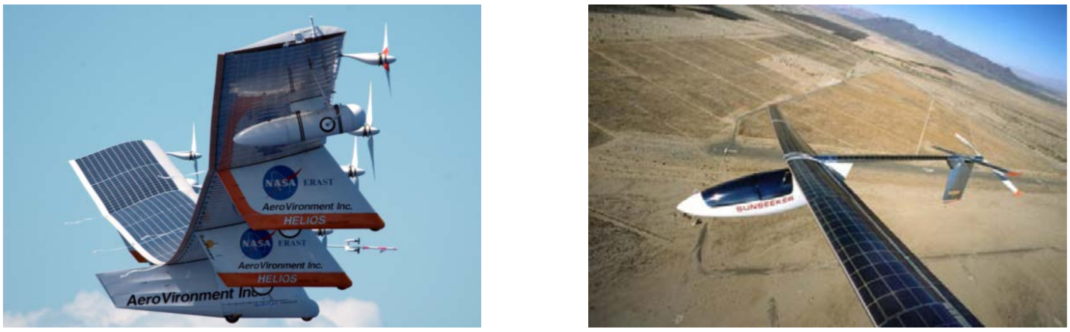

FIG. 2 Projects, a. Helios, b. Sunseeker

Developers in Australia (Parxis Aeronautics) have built a cSi-type flying wing UAV in the low-cost concept that has led to a six-year increase in performance, see FIG. 3 and 4.

FIG. 3. Flying wing –Parxis Aeronautics

FIG. 4. Flying wing Aquila – Facebook

Facebook has attempted to use the solar powered Aquila (2026) to provide Internet connectivity (relay relays) to areas of the world with no internet access [3].

2. PROPOSAL OF THE PHOTOVOLTAIC SYSTEM FROM THE UAV

The manufacturing of the flexible solar cell contains a compromise between efficiency, thickness, mechanical resilience and durability. The use of cells on lifting surfaces (wings, empennage) involves aerodynamics, elasticity and structure vibrations during flight, the main purpose of which is to ensure a safe battery loading on board.

The VTOL Flying Wing Concept contains three vectorized electric motors powered by a rechargeable electric source from a series of 20 interconnected photovoltaic cells placed on the load bearing surface, see Figure 5, [10, 11, and 12].

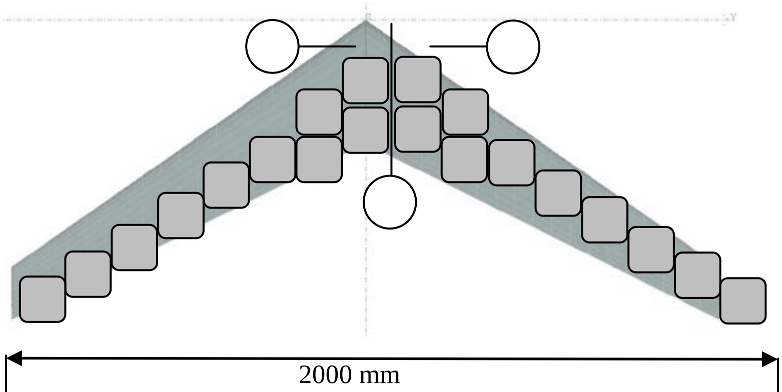

FIG. 5 FW-VTOL concept

The matrix of 20 photovoltaic cells will be mounted on a flying wing as in Figure 5. The system has been simulated software to demonstrate the efficiency of photovoltaic cell matrix. The circuit is complemented by a LiPo battery reassembly to make battery-to-battery shifting on charging versus charging.

The energy efficiency of the cell is given by the ratio between the maximum output power and the incidence of incidence radiation (E_v) on the cell, multiplied by the area A of the useful cell surface.

$$\eta = \frac{P_{max}}{E_v \cdot A} \cdot 100 \qquad (1)$$

The efficiency of photovoltaic panels is the ratio of power to the panel and power contained in total incident light.

$$\eta = \frac{P_{max}}{A \cdot G_a} \qquad (2)$$

Where:

P_{max} –Max power estimated

A- Illuminated surface

G_a – Solar irradiation

Although the wing has a total surface area of 0.5m2, it was initially desired to mount 30 flexible photovoltaic cells on the wing (figure 6), finally, the calculation of the surfaces allowed the installation of only 20 cells [13], so we have:

20 cells x 10 g= 200g (3)

The UAV's photovoltaic system provides the electrical power required for the operation of the propulsion system and radio-electronic equipment.

FIG. 6 Photovoltaic cell

The operating characteristics of photovoltaic cells are highlighted in Table 1 and FIG. 7.

Table 1 Characteristics of photovoltaic cells

Characteristics	Value	Characteristics	Value
Type	Si monocristalin	Efficiency	15%
Dimensions	125 x 125 mm	Mass	10 g
Thickness	165±40 µm	Max power P_{max}	3,46 W
Theoretical diameter	160 mm	Nominal power P_{nom}	3,45 W
Current	5,8 A	Voltage	0,57 V

FIG. 7a shows the characteristic I-U and FIG. 7.b shows the efficiency of the SunPower cell compared to the conventional photovoltaic cell and Solar Spectrum.

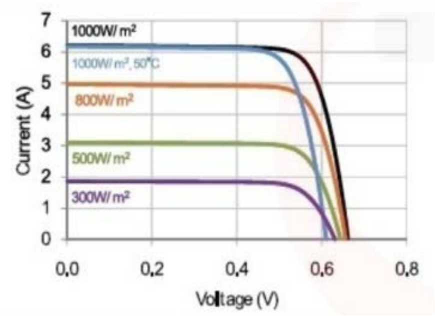

a

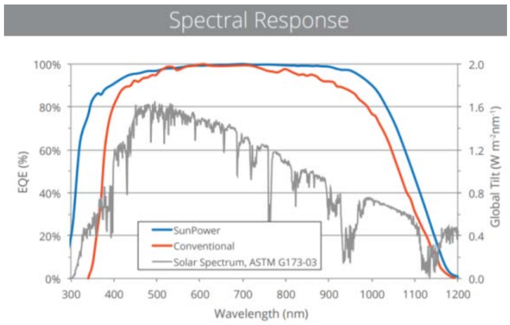

b

FIG. 7 Characteristics of photovoltaic cells, a. Current-Voltage, b. Efficiency versus wavelength

Configuration of photovoltaic system

In order to highlight the possibility of supplying a photovoltaic UAV, it was attempted to build an unmanned aerial platform, having on board this type of energy source, FIG. 8.

The proposed connections are highlighted in Figure 9 with only 20 photovoltaic cells. Starting from the requirements imposed by the radio-electronic installation and taking into account the extra mass that is added to the flywheel, it was decided to install a number of photovoltaic cells that would be able to supply the electric current required for the operation of the radio-electronic equipment, see Table 2.

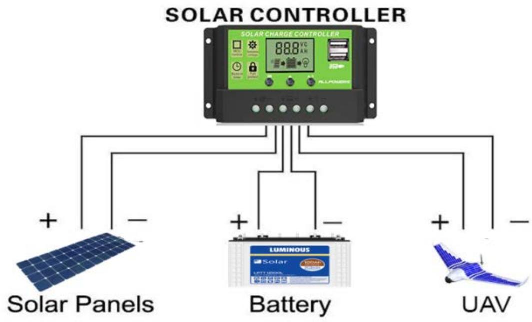

FIG. 8 The concept of FW-VTOL photovoltaic cell power supply

Table 2 FW-VTOL operating characteristics

Characteristics	Value	Characteristics	Value
Autopilot voltage/current	5,37 V / 2,25A	Voltage servo	4,8-6V
Controller electric motor, ESC	max 20A	Acc LiPo	11,1V, 2000mA
Battery eliminator circuit, BEC	5V		

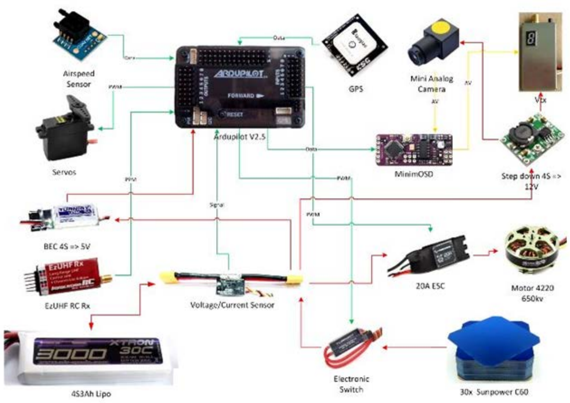

FIG. 9 System Connections

3. MEASUREMENTS AND SIMULATIONS ON THE PHOTOVOLTAIC SYSTEM

Measurements of the photovoltaic cell parameters

By successive measurements under various conditions and configurations we have found that the optimal solar cell coupling is in series providing an average output current of about 11V and 5.5A. I have verified the technical specifications of photovoltaic cells by exposing an office lamp with a 100-watt incandescent bulb. The results obtained are shown in Table 3.

Table 3 Measurement results

Cells number	**Voltage (V)**	**Current (A)**
1	0,55	5,3
10	5,4	5,4
20	10,6	5,4

To check the charge rate of the battery after unloading, I loaded it by exposing the photovoltaic cells to the 100W incandescent bulb lamp light, and using the Meter to monitor the charge rate (voltage differences) and the results are noted in Table 4.

Table 4 Results of measurements for loading times

Time (min)	**Voltage (V)**	**Time (min)**	**Voltage (V)**
10	2,85	49	3,38
23	2,99	68	3,57
37	3,09	79	3,60

Solar diagram simulation.

For 48^o parallel we have the solar diagram in Figures 10 and 11 [15].

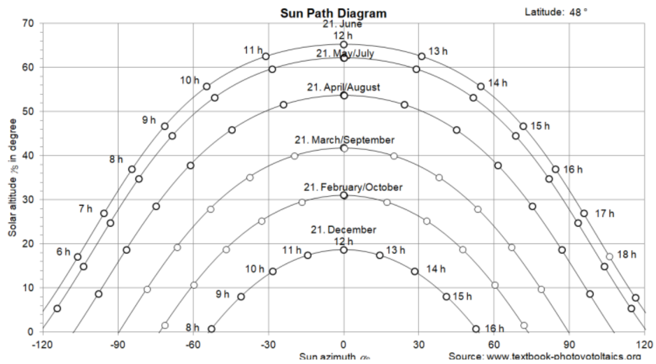

FIG. 10. Solar diagram for Romania

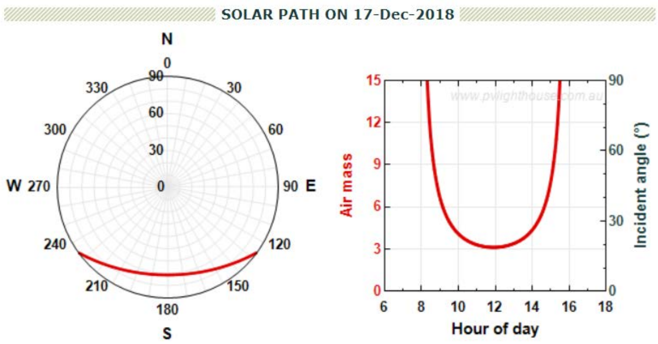

FIG. 11 The solar trajectory

FIG. 11 shows the value of the incidence of sun rays over a day, which influences the amount of battery charge depending on the time of flight. Simulation of the solar spectrum generates the numerical data in figure 12.

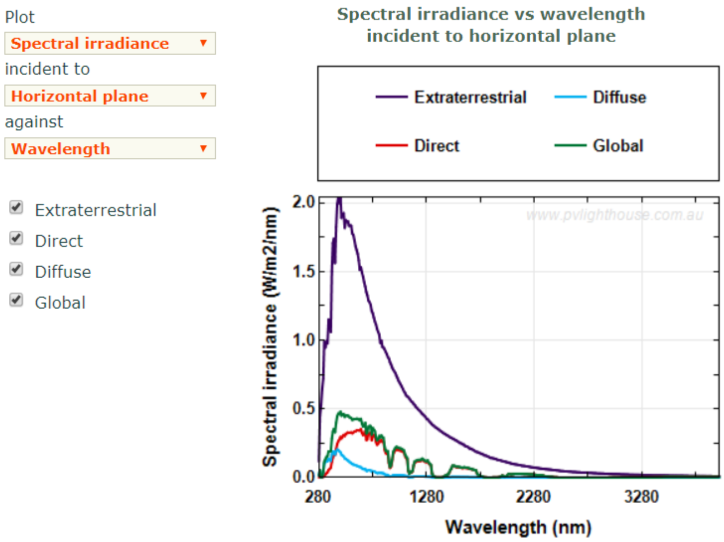

FIG. 12 Solar Spectrum

FIG. 12 shows the wavelength values (in a horizontal plane) depending on the radiant spectrum, we are mainly interested in the direct value (red curve) with a maximum at approx. 400 nm.

Simulation of photoelectric effect

A freeware Photoelectric Effect 1.01 was used, the results are Table 5 and FIG.13 [16].

Table 5 Light intensity

Nr. crt.	Light intensity (nm)	Voltage (V)	Nr. crt.	Light intensity (nm)	Voltage (V)
1	100	7,5	5	298	1,62
2	149	7,5	6	350	0,72
3	202	6,9	7	403	0,28
4	248	3,41	8	502	0

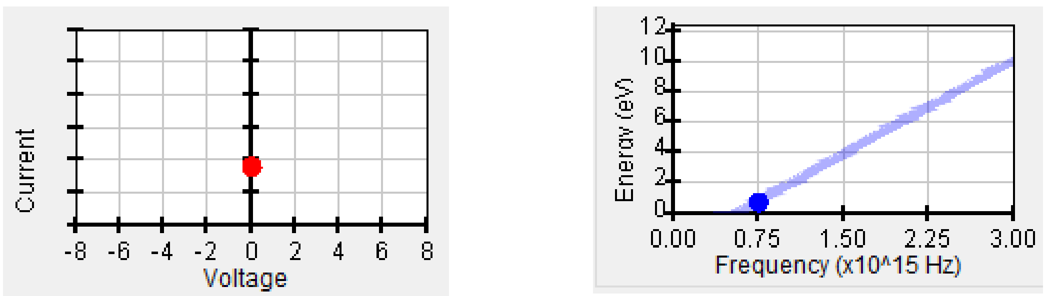

a b

FIG. 13 Photoelectric effect for 403 nm, a. Current-Voltage, b. Energy-frequency

The simulation considered a discharged LiPo battery and a 100% photon emission (unobstructed source).

Simulation of the equivalent circuit

Using the manufacturer's operating characteristics (Figure 14) for the equivalent circuit we generated the graphs in Figure 15 [15].

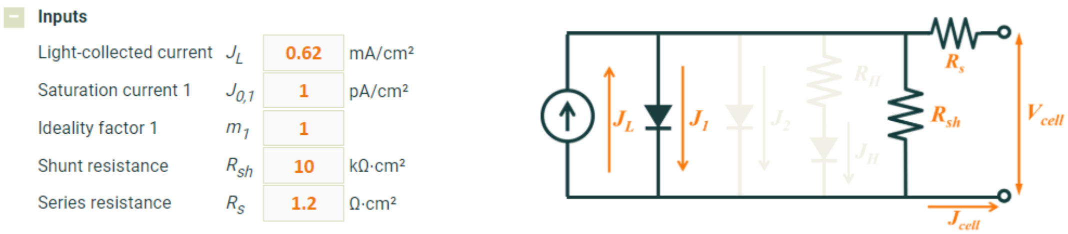

FIG. 14 Input data for the equivalent circuit

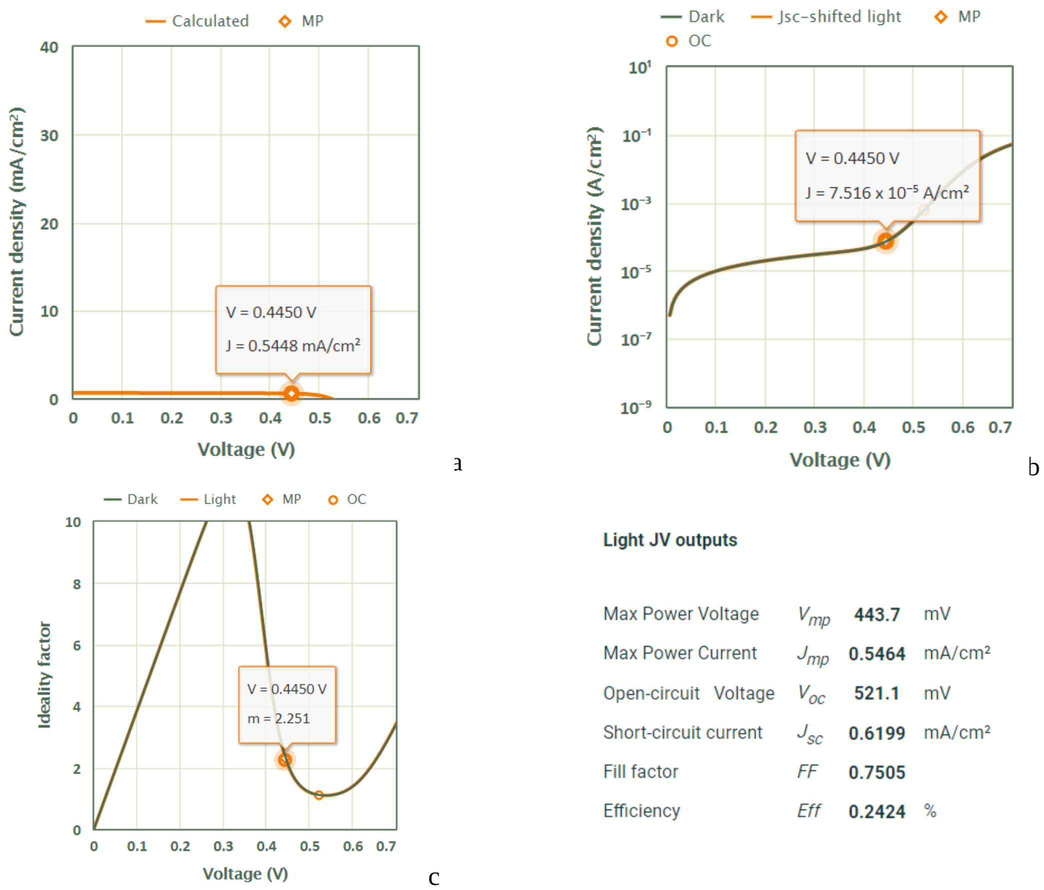

FIG. 15 Output data for the equivalent circuit

It can be seen from the simulation that the unit values of the cell voltage are lower compared to the values given by the manufacturer (0.57V vs. 0.44V) and the current 5.4A vs 5.8A.

CONCLUSIONS AND FUTURE RESEARCH

The global performances of UAV depend directly on the aerodynamic concept approached, the onboard equipment and the mode of operation by the human operator on the ground. The technical and tactical performances of UAV can directly affect mission quality with major influences on the acquisition, dissemination and decision-making capacity of data in the area of interest. Stability in the case of flying wing is achieved by selecting an optimal self-stabilizing profile, negative wing geometric torsion, or centring of the center of gravity below the center of gravity of the lifting surface.

The proposed photovoltaic system is an initial stage of study that can be put into practice with great success on FW-VTOL type UAVs over 3m span.

The article attempted to quantities the parts concerning: the pre-design of the photovoltaic system FW-VTOL and the characterization of the cell and solar module functioning characteristics by theoretical references and numerical simulations.

Future research should focus on the following main issues: building a complete 1:1 full scale benchmark (propulsion system, radio electronic system, retractable landing gear, photovoltaic system); making a demonstration model required for flight tests, scale 1:1 of 4m span; observing the aerodynamic behaviour of the FW-VTOL during the actual flight to create an optimized model; optimized model of the mass vs. the bearing surface and repetition of test processes under the conditions of using a optimized functional photovoltaic energy system.

REFERENCES

[1] Mermer Erdinç, *Conceptual design of a hybrid (turbofan/solar) powered HALE UAV.*, 2016, DOI 10.13140/RG.2.2.28805.65769., p.158;

[2] Dassault Systemes, *Aerospace and defence case study Solar Impulse*, https://www.3ds.com/fileadmin/customer-stories/SOLAR_IMPULSE_DS_HD.pdf, accessed at 12.01.2019;

[3] Aryan Kumar, Asha G. H., *AQUILA (THE SOLAR POWERED DRONE*), International Journal of Industrial Electronics and Electrical Engineering, ISSN: 2347-6982, Volume-4, Issue-10, Oct.-2016;

[4] Parvathy Rajendran, Muhammad Hazim Masral and Hairuniza Ahmed Kutty, Perpetual *Solar-Powered Flight across Regions around the World for a Year-Long Operation*, Aerospace 20/2017, vol.4; doi:10.3390/aerospace4020020, www.mdpi.com/journal/aerospace;

[5] Bennett, E. NASA's Helios prototype—Soaring to a new record. SAMPE J. 2002, 38, 41–47;

[6] https://www.nasa.gov/centers/dryden/images/content/86416main_ED03-0180-01.jpg, accessed at 12.02.2019;

[7] UAS Yearbook, *Unmanned aircraft systems – The Global Perspective 2011/2012*, Blyenburg & Co, June 2011, Paris, ISSN 1967-1709, 216 p., www.uvs-info.com;

[8] André NOTH, Design of Solar Powered Airplanes for Continuous Flight, 2008 Zurich, 196p, http://www.sky-sailor.ethz.ch/docs/Conceptual_Design_of_Solar_Powered_Airplanes_for_continuous_flight.pdf;

[9] https://reneweconomy.com.au/father-son-australian-company-develops-solar-powered-drone-46232/, accessed at 22.02.2019;

[10] Prisacariu V., *Performance analysis of the flying wing airfoils*, RECENT Journal 1(51)/2017, vol 18, Transilvania University of Brasov, Romania, ISSN 1582-0246, p. 56-63;

[11] Prisacariu V., Cîrciu I., *The analysis of the flying wing in morphing concept*, INCAS Bulletin, vol.5, issue 2/2013, p43-52, ISSN 2066-8201, Bucuresti;

[12] *** *Guidelines for XFLR5 v6.03*, 2011, 71p.;

[13] https://us.sunpower.com/sites/sunpower/files/media-library/spec-sheets/sp-sunpower-maxeon-solar-cells-gen2.pdf, accessed at 02.02.2019;

[14] *Solar powered APM plane that charges your batteries as you fly,* https://blog.dronetrest.com/solar-powered-apm-plane-that-charges-your-batteries-as-you-fly/, accessed at 22.03.2019;

[15] https://www2.pvlighthouse.com.au/calculators/solar%20path%20calculator/solar%20path%20calculator.aspx, accessed at 10.03.2019;

[16] *Photoelectric Effect 1.01,* https://phet.colorado.edu/en/simulation/photoelectric, accessed at 09.02.2019.